JOURNAL OF MATERIALS SCIENCE 28 (1993) 3564–3570

Fracture mechanics of blunt cracks in a ductile steel

E. H. ANDREWS, M. A. ANSARIFAR*
Department of Materials, Queen Mary and Westfield College, Mile End Road, London E1 4NS, UK

The propagation of blunt notches in stainless steel has been studied experimentally and analysed using generalized fracture mechanics (GFM), which takes account of inelastic and non-linear deformation. According to this theory, the critical apparent energy release rate, which is equivalent to J_c, is given by $J_c = k_1(\varepsilon_0)\, c W_{0c}$ for an edge crack of length c in a thin sheet (plane stress), where $k_1(\varepsilon_0)$ is a dimensionless function of strain, ε_0, and W_{0c} is the input energy density remote from the crack at the time of crack propagation. The validity of this equation was demonstrated for blunt cracks and the function $k_1(\varepsilon_0)$ evaluated. The value of J_c was measured for blunt cracks of different lengths and tip diameters, and also for different crack extensions. J_c was found to be independent of crack length for the smallest tip radius, but became systematically length-dependent as the radius increased. However, the dependence of J_c on crack length, tip radius and crack extension can be expressed by a single empirical function, as is suggested by GFM. The propagation of cracks from blunt notches in ductile materials can, therefore, be handled by fracture mechanics methods.

1. Introduction

Almost by definition, fracture mechanics analysis is restricted to the propagation of sharp cracks. One reason for this is that the crack-tip radius is assumed to be effectively zero when the relevant equations are derived and does not, therefore, feature explicitly in those equations. Those formulations of fracture mechanics that are based upon energy balance, assume that an energy release rate in excess of the critical value is a sufficient condition for propagation, and this is only true as tip radius tends to zero. Equally, stress-field parameters like K_c are based upon the stress distribution around a zero-radius crack. It is true that "crack blunting" is considered when discussing R-curves or when using Dugdale or crack opening displacement (COD) analyses [1], but it is not generally possible to retain geometry independence in the fracture mechanics parameters unless the crack is sharp. Consequently, the propagation of cracks which are blunt before the specimen is loaded has received little attention.

This does not mean, however, that the subject is of no interest. Any crack propagating in a ductile solid must eventually become blunt, even if it was originally sharp, and this is particularly true of fatigue cracks. Similarly, if the solid is inhomogeneous on a coarse scale, as in a composite for instance, crack propagation is always "blunt" rather than "sharp". Finally, the tearing of ductile materials from holes or notches is an example of blunt crack propagation and could have significance in engineering design and safety assessment.

We have therefore studied the energy required to propagate blunt edge cracks or notches in plane stress (i.e. using thin sheets) as a function of crack length, tip radius and crack extension, and have sought to analyse the results using generalized fracture mechanics. This allows us to derive a J_c value for each combination of the variables employed and to rationalize the dependence of J_c upon those variables.

2. Experimental procedure

2.1. Materials and specimen preparation

The material used in these experiments was an 18/8 stainless steel of composition C 0.05%, Si 0.36%, Mn 1.57%, S 0.02%, P 0.03%, Ni 9.28%, Cr 17.5%, Nb 0.69%, remainder Fe.

The steel was supplied as cold-rolled, softened and descaled sheet, approximately 0.91 mm thick.

Wide dumb-bell specimens, 150 mm long by 50 mm wide, were cut out of the sheet with their long axes in the rolling direction. Single-edge notches of various lengths were machined into the dumb-bells half-way along their length and perpendicular to the tensile axis (see Fig. 1). Each notch was terminated with a drilled hole of specified radius to provide a well-characterized "blunt crack". Specimens were divided into five sets according to their crack-tip diameters, D. The bluntness of the cracks and the ductile nature of the steel ensured that propagation occurred only by slow controlled tearing of the material.

To facilitate the study of "resistance curve" effects, a series of lines was engraved on each specimen at 1 mm intervals ahead of, and perpendicular to, the

* *Present address*: The Malaysian Rubber Producers' Research Association, Brickendonbury, Hertford, SG13 8NL, UK.

0022–2461 © *1993 Chapman & Hall*

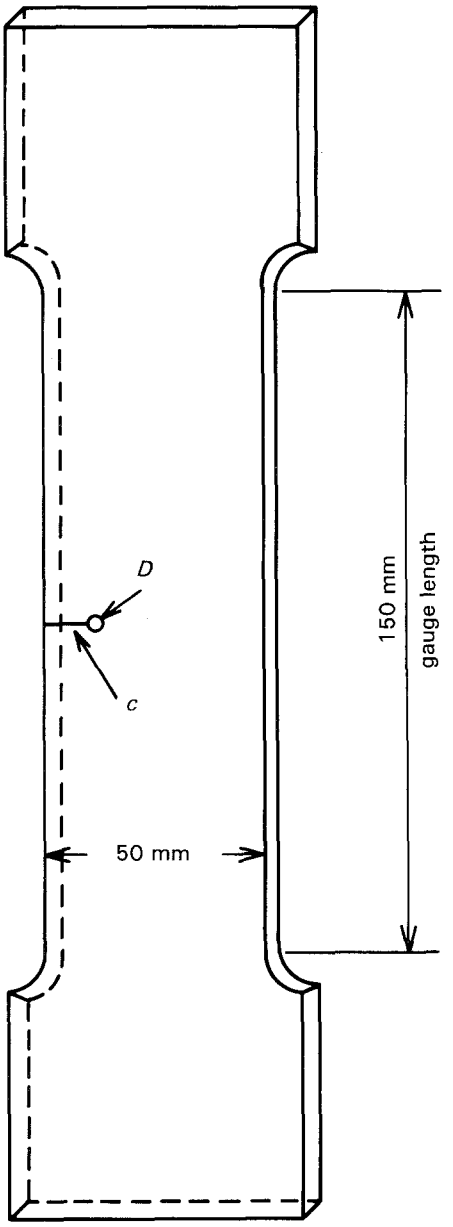

Figure 1 Test specimen showing edge crack and tip diameter.

crack. This allowed the operator to activate an "event marker" to mark the load–deflection curve at the moment the propagating crack crossed each engraved line.

2.2. Variables studied and procedure

Five different tip diameters were employed, ranging from 0 (fatigue crack)–2.0 mm. This gave five sets of specimens, each set having a single tip diameter. For each tip diameter (except zero) a range of initial crack lengths was employed, from 5–15 mm. The details are given in Table I. Each set also contained an un-notched control specimen.

The edge-notched dumb-bell specimens were deformed monotonically in tension in an Instron Universal Testing Machine at a crosshead speed of 0.5 mm min^{-1} and the load–deflection curve recorded in the normal way. The propagation of the crack was observed through a cathetometer and the event marker actuated each time the propagating tip crossed an engraved line. A typical set of stress–strain curves obtained in this manner is shown in Fig. 2.

TABLE I Table of specimen dimensions

Set	Crack-tip diameter (mm)	Crack lengths (mm)					
1	0.0 (fatigue crack)	–	–	–	–	–	15.0
2	0.5	0.0	5.0	7.5	10.0	12.5	15.0
3	1.0	0.0	5.0	7.5	10.0	12.5	–
4	1.5	0.0	5.0	7.5	10.0	12.5	15.0
5	2.0	0.0	5.0	7.5	10.0	12.5	15.0

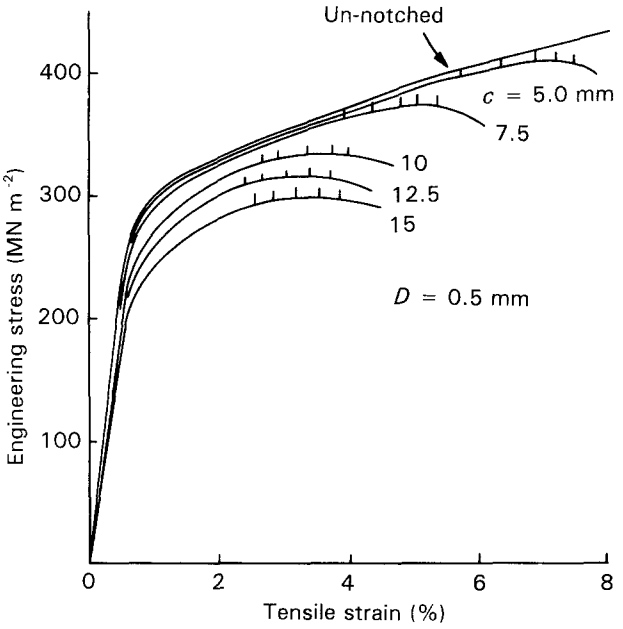

Figure 2 Typical stress–strain curves for a set of edge-notched specimens with cracks of different lengths, c. Vertical marks show onset of crack growth and successive 1 mm increments of crack extension.

3. Analysis and presentation of experimental data

3.1. Evaluation of the function $k_1(\varepsilon_0)$

Generalized fracture mechanics (GFM) gives the following equation for the "apparent energy release rate" [2]

$$-(dE/dA) = k_1(\varepsilon_0) c W_0 \quad (1)$$

where E is total energy, A is crack area, $k_1(\varepsilon_0)$ is a function of the strain, ε_0, remote from the crack, c is the crack length, and W_0 is the input energy density remote from the crack.

Integrating this equation at constant ε_0, W_0, we obtain

$$-\Delta E = k_1(\varepsilon_0) h W_0 c^2 \quad (2)$$

where h is the sheet thickness and ΔE is the input energy difference (at constant load) between the specimen containing a crack and the un-notched control specimen. This energy difference is obtained from the load–extension curve (not the stress–strain curve) by measuring the area between the respective curves for notched and un-notched specimens up to any selected load value (see Fig. 3). By choosing different load values, ΔE can be found as a function of load. The area under the load–extension curve of the un-notched specimen, up to each selected load, when divided by

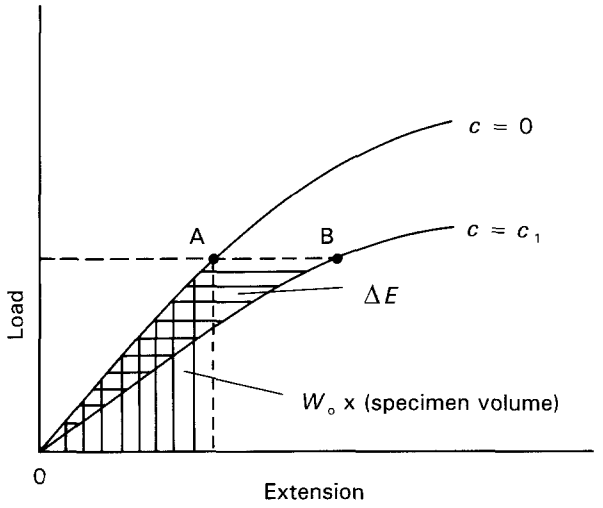

Figure 3 Calculation of energy change with respect to crack length.

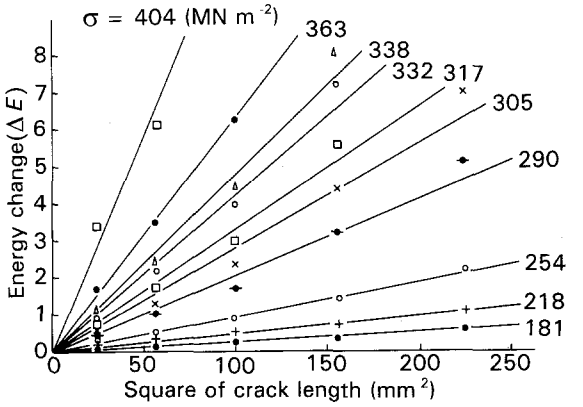

Figure 4 Energy change at different stress levels as a function of the square of crack length, for 2.0 mm crack-tip diameter, showing linear dependence.

the specimen volume (i.e. gauge length × width × thickness), is the appropriate value of W_0. Thus, all the terms in Equation 2 are known with the exception of $k_1(\varepsilon_0)$. The strain, ε_0, has a one-to-one relationship to W_0, because both refer to the homogeneously deformed region remote from the crack. This relationship is therefore found from the stress–strain curve of the un-notched control specimen allowing a value of ε_0 to be assigned for each value of W_0.

The ΔE value is conveniently found by cutting out and weighing the piece of graph paper defined by the area OAB in Fig. 3 and calibrating by reference to the weight of a known area (corresponding to a known energy) cut from the same sheet of paper.

According to Equation 2, a plot of ΔE against c^2 should give a straight line through the origin with a slope $k_1(\varepsilon_0)hW_0$. There will be a different line for each different load (and thus for each different W_0 value). An example of such data is shown in Fig. 4. At the highest loads, fewer points are available because specimens with longer cracks have already fractured. At the highest crack lengths and intermediate loads there is a tendency for ΔE to be too high. However, having regard to the possible sources of experimental error, especially specimen to specimen variability, a linear relationship provides a good approximation even in the worst cases. For lower loads

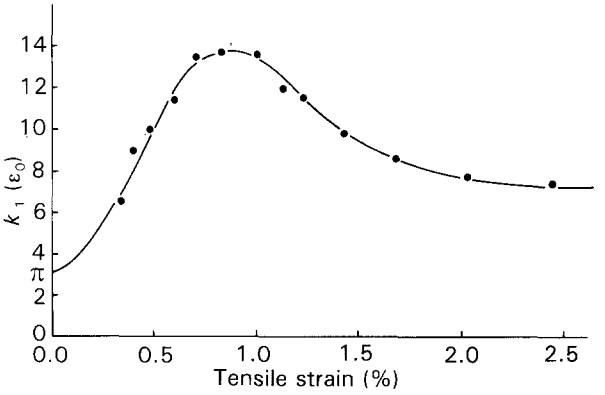

Figure 5 The function k for $D = 1.5$ mm as a function of strain remote from the crack.

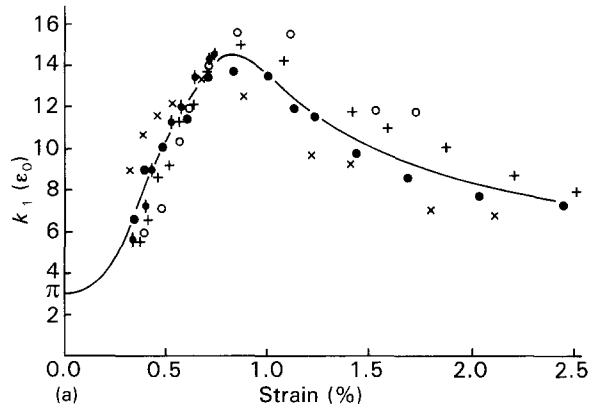

Figure 6 As Fig. 5 but for all crack-tip diameters, D: (●) 0, (×) 0.5 mm, (○) 1.0 mm, (●) 1.5 mm, (+) 2.0 mm.

(or W_0 values) and for shorter cracks, the linearity is very good.

From the slopes of the lines in Fig. 4 and the known values of W_0 and h, it is possible to derive $k_1(\varepsilon_0)$ as a function of W_0 and therefore of strain ε_0. An example of this functionality is given in Fig. 5. At infinitesimal strain, $k_1(\varepsilon_0)$ should tend to a value of π as shown [2]. As observed previously for ductile metals [3] and various plastics and rubbers [4], the function $k_1(\varepsilon_0)$ rises from its infinitesimal strain value to a peak and then decays slowly with further strain. The peak strain corresponds to the yield point in the stress–strain curve.

In Fig. 6 we have superimposed the $k_1(\varepsilon_0)$ data from all five sets of specimens (that is, all five tip diameters). There is some scatter but no systematic trend with tip diameter and we conclude, therefore, that the function $k_1(\varepsilon_0)$ is not sensitive to tip diameter. For the critical case we then have

$$J_c = k_1(\varepsilon_0) c W_{0c} \quad (3)$$

3.2. Deriving J_c and J_R

By definition, J_c is the critical value of the energy release rate at the point of propagation and J_R is its value at any defined point during subsequent propagation. It is, therefore, possible (from Equation 3) to obtain these J parameters as the slopes of plots of

$k_1(\varepsilon_0) W_{0c}$ against reciprocal crack length, where W_{0c} is the appropriate value of W_0 at the moment of interest (e.g. onset of propagation or some given crack extension). "Crack length" includes the crack extension in these and subsequent plots.

Fig. 7 show two such plots for the case where $D = 0.5$ mm and crack extension Δc is (a) zero (the initiation case) and (b) 1 mm, respectively. Fig. 7a, where there is no crack extension, gives an excellent straight line through the origin, as expected from the theory. By contrast, Fig. 7b, with 1 mm crack extension, appears to demonstrate a deviation from linearity. This trend is confirmed by the results for the same crack radius but even larger crack extensions of 2, 3 and 4 mm (Fig. 8a–c). In Fig. 8 we have not attempted to draw a straight line through the origin, but instead have connected each point to the origin by its own line. Remembering that the slope of each plot in Figs 7 and 8 equals the relevant value of J, this means that we are attributing the non-linearity of the plots to a variation of J_c or J_R with crack length. The implied dependence upon crack length increases from no dependence at zero crack extension, to a maximum at the highest crack extension of 4 mm.

In earlier publications, where crack radius was not a variable, the non-linearity demonstrated in Fig. 8 was attributed to a finite-width effect [3, 5]. That is, the curve was held to be linear, giving constant J_c and a positive intercept on the abcissa which was interpreted as the reciprocal width of the specimen. This seemed reasonable at the time, because the theory applies to an infinite plate and some finite-width correction will be required for large crack length. In the light of the present work, however, we now believe that this was a misinterpretation, and that the non-linearity of the curves in Fig. 8 arises from a genuine dependence of J_c, J_R upon crack length when non-zero crack radius is combined with non-zero crack extension. As we shall see, this conclusion is forced upon us by the increasing deviation from linearity observed as the radius gets larger.

An alternative, of course, would be to say that the theory no longer applies under these conditions. However, as we shall see, GFM actually predicts a dependence of J_c, J_R upon length for non-zero crack radius and crack extension, so that we proceed to derive crack-length dependent values for the J parameters.

To complete the picture, Figs 9–11 give the data for tip diameters 1.0, 1.5 and 2.0 mm, showing the progressive deviation from linearity with rising diameter and crack extension. For the sake of clarity in these plots, we have not joined each point to the origin but have joined points for the same Δc by broken lines to indicate trends.

Fig. 12 shows data for zero crack diameter (fatigue cracks), which were only obtained for a single crack length, namely 15 mm. Again joining each point to the origin to obtain a J value, we observe the familiar "resistance curve" effect in which J_R rises with increasing crack extension until it levels off at an extension of 3–4 mm.

It is, of course, possible to provide various cross-plots of the data for J to give, for example, R-curves at

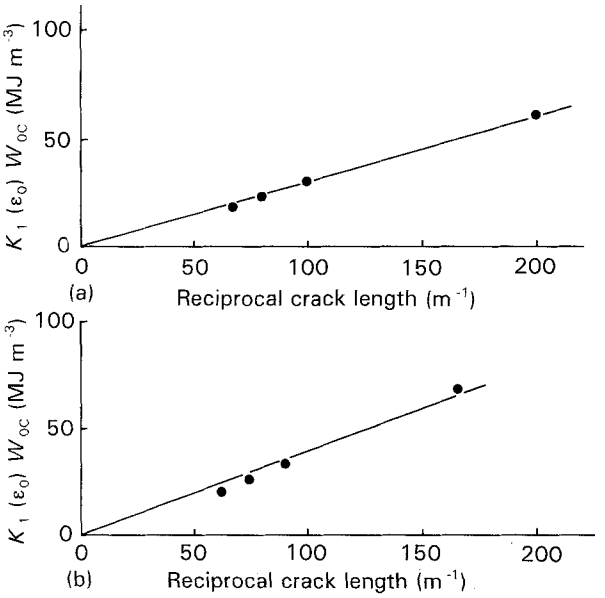

Figure 7 Plot based on Equation 3 for crack-tip diameter of 0.5 mm. The slope of the line gives J_c or J_R. (a) Crack initiation, (b) crack extension of 1 mm.

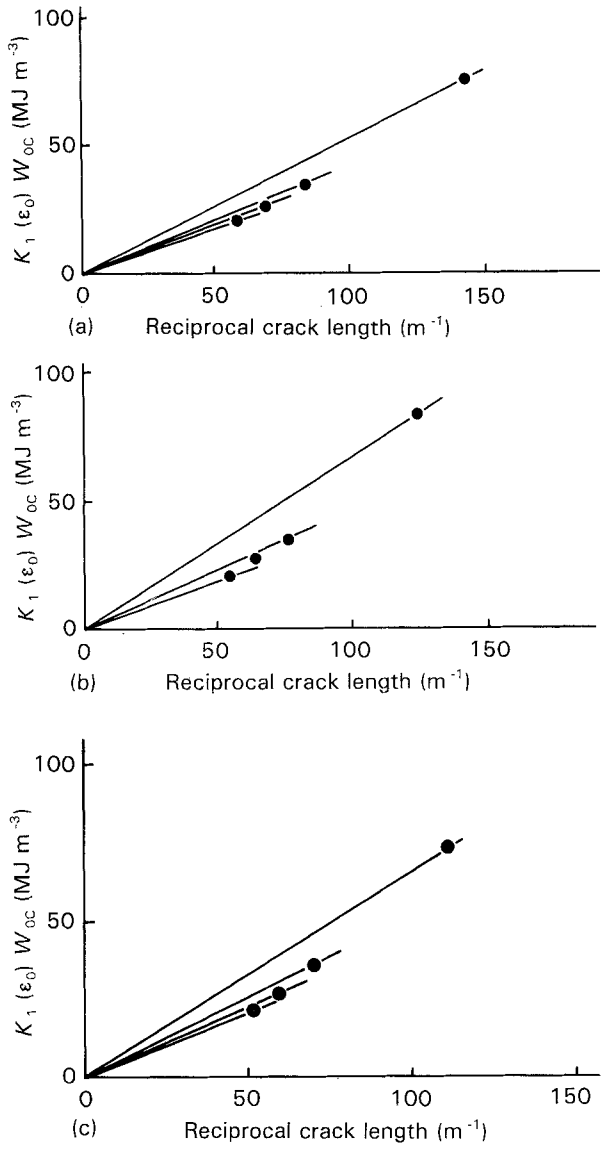

Figure 8 As Fig. 7, but for other crack extensions of (a) 2.0 mm, (b) 3.0 mm, and (c) 4.0 mm. Note the increasing departure from linearity as crack extension increases.

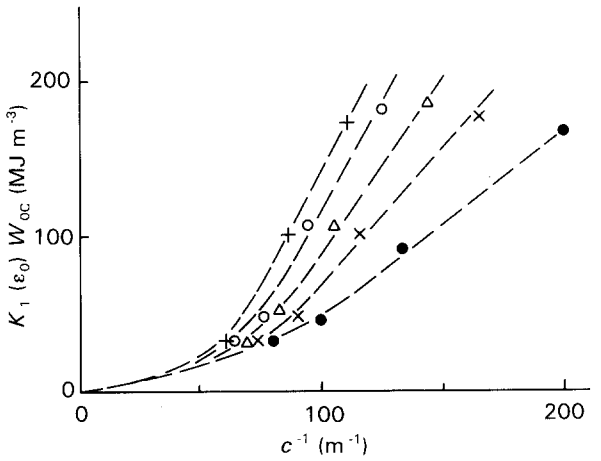

Figure 9 As Fig. 7, but for tip diameter of 1.0 mm, and different crack extensions: (●) 0, (×) 1 mm, (△) 2 mm, (○) 3 mm, (+) 4 mm. Note the increasing departure from linearity as diameter and crack extension increase.

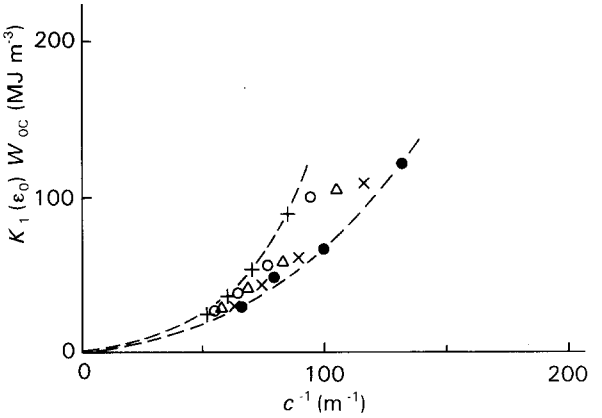

Figure 10 As Fig. 7, but for tip diameter of 1.5 mm, and different crack extensions: (●) 0, (×) 1 mm, (△) 2 mm, (○) 3 mm, (+) 4 mm. Note the increasing departure from linearity as diameter and crack extension increase.

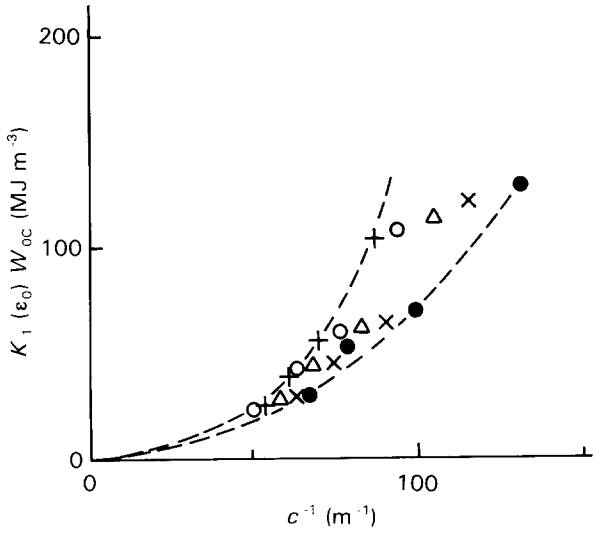

Figure 11 As Fig. 7, but for tip diameter of 2.0 mm, and different crack extensions: (●) 0, (×) 1 mm, (△) 2 mm, (○) 3 mm, (+) 4 mm. Note the increasing departure from linearity as diameter and crack extension increase.

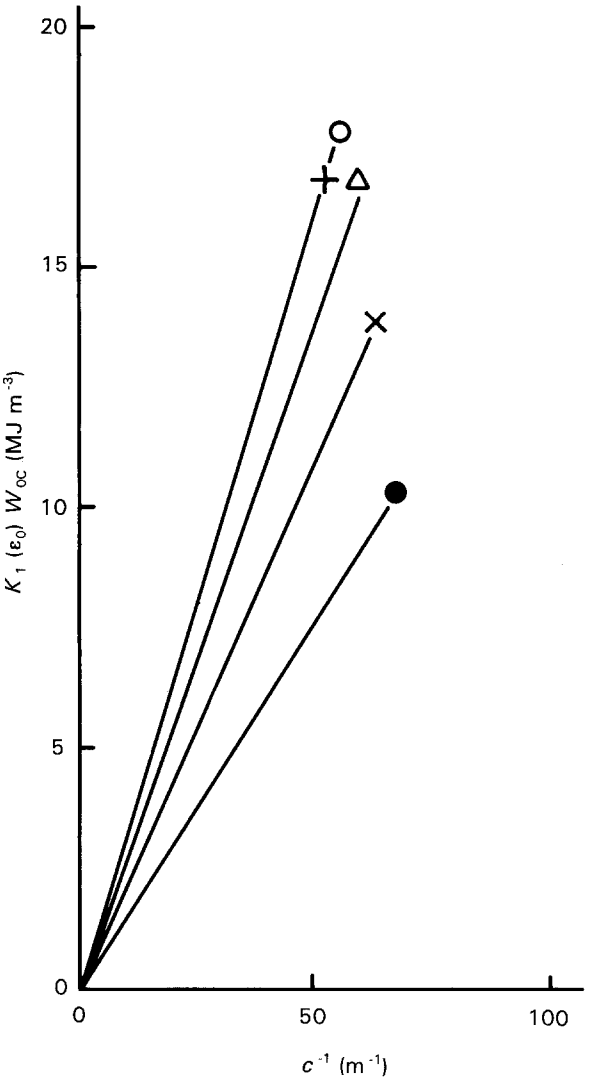

Figure 12 As Fig. 7, but for only one crack length, zero tip diameter and different crack extensions: (●) 0, (×) 1 mm, (△) 2 mm, (○) 3 mm, (+) 4 mm. Each point is joined to the origin to provide a separate J value for each crack extension.

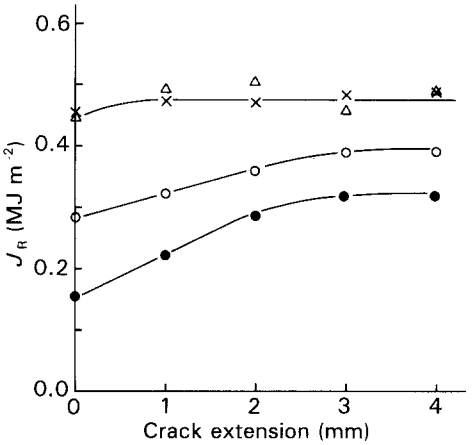

Figure 13 Resistance curves for different tip diameters, D: (△) 2.0 mm (×) 1.5 mm, (○) 0.5 mm, (●) 0.

each tip diameter. Several such curves are seen in Fig. 13, where the dependence of J_R on diameter and crack extension is made explicit. Equally J_R is plotted, for a fixed crack diameter of 0.5 mm, against crack length for five different crack extensions in Fig. 14.

4. Discussion and further analysis of the results for J_R

It is clear from Figs 8a and 14 that the results tend to those expected as both tip diameter, D, and crack extension, Δc, tend to zero. That is, J_R is independent

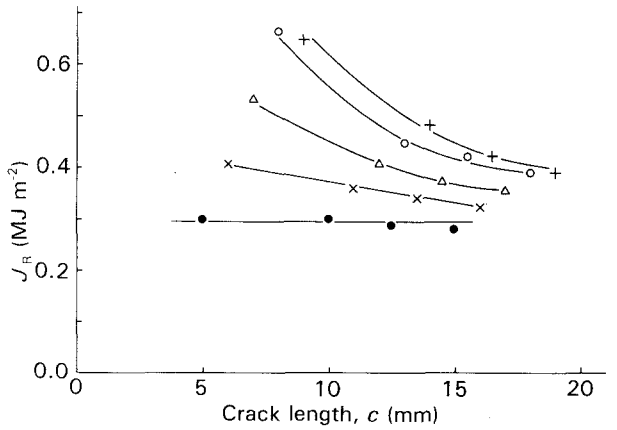

Figure 14 Effect of crack length and crack extension on the value of J_R for $D = 0.5$ mm. Δc: (●) 0, (×) 1 mm, (△) 2 mm, (○) 3 mm, (+) 4 mm.

of crack length for small D (say, 0.5 mm and below) and small crack extension, Δc (say 1.0 mm and smaller). For $D = 0.5$ mm, an effect of crack length upon J_R begins to appear at short crack lengths when the crack extension is large. If we only had data for this diameter (or smaller) we might dismiss these crack-length effects as experimental scatter. As we move to larger crack diameters, however, it becomes increasingly obvious that J_R is no longer independent of crack length and that the R-curve phenomenon becomes more severe as the tip diameter rises.

The question arises as to whether J_R retains any physical significance under these conditions. We believe that the systematic nature of the dependencies of J_R upon the geometrical parameters of crack length, tip diameter and crack extension suggest that it does retain such significance, and that the significance follows naturally from the GFM formulation of fracture mechanics.

In the derivation of Equation 3, GFM begins by expressing the input energy density at a point P in the stress field, as [2]

$$W(P) = W_0 f(X/c, Y/c, a/c, b/c, d/c, \ldots) \quad (4)$$

where X, Y are the co-ordinates of point P; a, b, d, etc. are available dimensions of the specimen; and c is a selected dimension, usually (but not necessarily) the crack length. Usually, for simplicity, we specify that the specimen is an infinite sheet of uniform thickness containing a centre crack of length $2c$. This means that the only available dimension other than c is the thickness. For plane strain or plane stress extremes, we may further simplify by making the thickness infinite or tending-to-zero as the case may be. This leaves no available dimension other than the crack length, so that all terms vanish from the bracket in Equation 4 except those involving the co-ordinates X and Y.

On the other hand, if there are available dimensions in the system, such as a non-zero crack-tip diameter, and a non-zero crack extension, it is clear that they must affect the value of the function f (though we cannot tell theoretically in what manner).

The function f carries through into the final expression for J_c or J_R in the following form [1], where, for conciseness, J_c also represents J_R

$$J_c = J_0 \Phi(a/c, b/c, d/c \ldots) \quad (5)$$

where J_0 is some minimum crack propagation energy and Φ is the "loss function". The function, f, is involved because Φ contains terms of the form df/dx and df/dy. For our present purpose, it is convenient to make J_0 the J-value for $D = 0$ and $\Delta c = 0$.

We see, therefore, that J_c can only be expected to be independent of crack length if all dimensions of the specimen other than crack length, are zero or infinite (and thus "unavailable" for dimensional analysis). For non-zero tip diameter we shall expect terms in D/c to be present in Φ, and for non-zero crack extension, terms in $\Delta c/c$.

Thus, in general, we would expect

$$J_c = J_0 G(D/c, \Delta c/c) \quad (6a)$$

Alternatively, this is equivalent to

$$J_c = J_0 H(D/c, \Delta c/D) \quad (6b)$$

where G, H are functions, with the further proviso that the new functions G and H must tend to unity when D and Δc both tend to zero, leaving J_c equal to its basic value J_0 for sharp cracks and zero crack extension.

A possible explicit form of Equation 6 is

$$J_c - J_0 = A(n + [D/c])^p \times \{m + [\Delta c/(D + e)]\}^q \quad (7)$$

where n is a constant to prevent $J - J_0$ going to zero at zero D and non-zero Δc, m is a constant to prevent $J - J_0$ going to zero at zero Δc and non-zero D, e is a constant to prevent $J - J_0$ going to infinity at zero D, and p and q are further constants.

The form of the function chosen is not altogether arbitrary. The constants n, m and e are required by the boundary conditions, and only their values remain adjustable. The exponents p and q simply recognize that there is no reason to expect linearity in either the diameter-dominated or the extension-dominated term.

Using a process of trial and error, facilitated by a spreadsheet plotting facility (Quattro Pro by Borland), it was possible rapidly to run through a range of possible values for n, m, e, p and q, to see which values would allow all data points, for all crack lengths, tip diameters and crack extensions, to be displayed as a single curve.

The best fit we have been able to find, without departing from the basic simplicity of Equation 7, is to set the various constants to the following values: $J_0 = 234\ \mathrm{J\,m^{-2}}$, $A = 1.6\ \mathrm{J\,m^{-2}}$, $n = 0.1$, $m = 4.0$, $e = 0.5$ mm, $p = 1.5$, $q = 2.5$.

In principle, J_0 is an experimentally measured parameter, namely the J_c value for zero diameter (sharp) cracks. This value was $155\ \mathrm{J\,m^{-2}}$, but the higher value of $234\ \mathrm{J\,m^{-2}}$ has been chosen to improve the fit between theory and experiment overall.

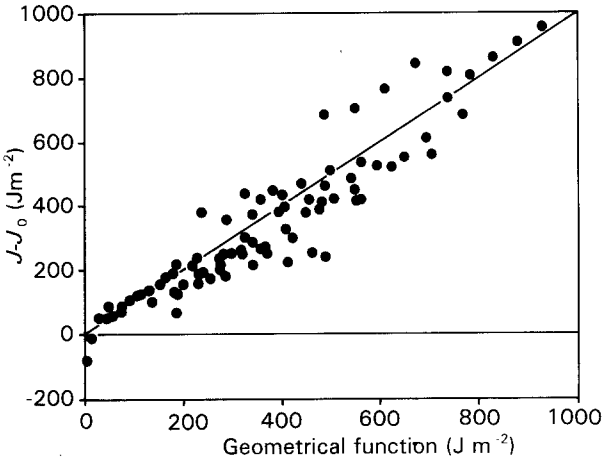

Figure 15 Plot of J–J_0 against the geometrical function of Equation 8, showing that J_c values for all crack lengths, diameters and crack extensions can be described by a single function of the geometrical variables.

Fig. 15 is a plot of $(J_c - J_0)$ $(\mathrm{J\,m^{-2}})$ as ordinate against the "geometrical function"

$$1.6(0.1 + [D/c])^{1.5}\{4 + [\Delta c/(D + 0.5)]\}^{2.5} \quad (8)$$

using the adjustable parameter values given above. It will be seen to represent the total data collection to a fair approximation over the whole range of variables. Although the geometrical function (Equation 8) does not go precisely to zero for zero D and Δc, its value under these conditions is negligible when compared with other conditions.

It should be emphasized that the geometrical function chosen is not necessarily the only, or best, function to represent the data. What it does demonstrate is that the variation of J with the variables of crack length, tip diameter and crack extension, can plausibly be represented by a single, rational, non-dimensional function of those variables, and with one-to-one linearity.

5. Conclusion

The fracture mechanics parameter J_c can be defined, and therefore measured, for the propagation of blunt notches or cracks using generalized fracture mechanics. J_c exhibits normal "crack resistance" effects, rising with crack extension, but is only independent of crack length for zero crack-tip diameter.

When the crack-tip diameter is non-zero, there is a complex but systematic dependence of J_c upon crack length, tip diameter and crack extension. To a fair degree of approximation, this complex dependence can be represented by a single function of the non-dimensional geometrical variables which has a simple form.

This work therefore emphasizes the role of the geometrical variables in determining J_c for a given ductile material. These variables exert their influence in non-dimensional forms, namely as the ratios of the "available dimensions" of the specimen. Thus it becomes possible to extend fracture mechanics treatments to cases which have not previously been amenable to this form of analysis.

References

1. D. G. H. LATZKO, "Post-yield fracture mechanics" (Applied Science, London, 1979) pp. 28, 211.
2. E. H. ANDREWS, *J. Mater. Sci.*, **9** (1974) 887.
3. E. H. ANDREWS and E. W. BILLINGTON, *ibid.* **11** (1976) 1354.
4. E. H. ANDREWS and Y. FUKAHORI, *ibid.* **12** (1977) 1307.
5. E. H. ANDREWS and J. I. BHATTY, *Int. J. Fract.* **20** (1982) 65.

Received 10 April 1992
and accepted 4 January 1993